2008: The Journal of Astronomical Data 14, 3.

Emission Lines in 32 Cygni

Joel A. Eaton
Center of Excellence in Information Systems, Tennessee State University,
Box 9501, 3500 John A. Merritt Blvd., Nashville, TN 37209, USA

Received 08 September 2008; accepted 05 November 2008

Abstract

I identify the profusion of emission lines seen in *IUE* spectra of 32 Cyg (K4-5 Ib+B6-7 IV-V) during total eclipse. With the exception of a very few weak lines, all of these are also seen in ζ Aur during its eclipse, and the stronger features appear in 31 Cyg. Seventy-four percent of these emission lines can be attributed to Fe II. Few are intrisically weaker than $gf \sim 0.01$. Other spectra definitely present are C II, N I, O I, Si II, Mg II, S II, Cr II, Ni II, Al II, Al III, Fe III, Si IV, and C IV. No emission lines of the neutral metals, except for fluorescent Fe I UV44, are unambiguously detected; specifically, lines of C I, Si I, or S I were not detected in the spectrum.

1 Introduction

The ζ Aur binaries (Wright 1970) provide a laboratory for studying wind structure in cool evolved stars. The hot B-dwarf companions of the K supergiants in typical systems move through and behind the wind of the cool star, interacting with it and giving us clues about its structure (e.g., Wilson & Abt 1954). Common ions in the wind scatter light from the hot star and produce a rich emission-line spectrum seen in total eclipse (e.g., Chapman 1981; Eaton & Bell 1994; Baade et al. 1996; Bauer et al. 2008). Analyses of the winds of three stars, ζ Aur, 32 Cyg, and 31 Cyg, by Che et al. (1983) have shown that profiles of lines scattered in the wind can be used to determine mass loss rates for them, typically near 10^{-8} $M_\odot$ yr^{-1}. Analyses of absorption during atmospheric eclipses also give mass loss at this level (e.g., Eaton 1993; Eaton & Bell 1994; Baade et al. 1996).

Because of the low electron densities expected in chromospheres and winds of cool giants, almost all the processes forming the emission lines will be scattering (Judge et al. 1992). This ensures a much richer spectrum than would be expected of a gas emitting thermally at $\sim$ 10,000 K. Consequently, very few of the *intrinsic* emission lines seen in ultraviolet spectra of single giants (see, e.g., McClintock et al. 1975; Judge 1986; Judge

& Jordan 1991) can be detected in these binaries. The normally rich Fe II spectrum, for instance, is completely overwhelmed by the shell emission.

In this paper I identify the emission lines in the eclipse spectrum of 32 Cyg and discuss the mechanisms of their formation. 32 Cyg is especially good for cataloguing the scattered shell lines because it has the most intense spectrum of the three classical ζ Aur binaries. See Eaton (1993) for a discussion of the spectral classification of the stars and an analysis of the *IUE* observations of atmospheric eclipse; see Eaton et al. (2008) for an analysis of the ellipsoidal light variation of the K star. I give the line identifications in Section 2, then disuss the nature of the spectrum and its context in Sections 3 and 4.

2 Observations

The observations analyzed consist of a pair of deeply exposed *IUE* spectra of 32 Cyg taken in total eclipse on 31 March 1981 by R. E. Stencel. Spectrum SWP13623 covers 1180–1950 Å, LWR10255, 2100–3200 Å. Exposure times were four hours and one hour, respectively. The actual data incorporate the standard reductions in use when the spectra were taken; they were obtained from the *IUE* project at NASA Goddard Space Flight Center. Figure 1 shows the combined eclipse spectrum. I have also compared the data for 32 Cyg with spectra of ζ Aur (a composite of all the 8 *IUE* spectra recorded in total eclipse) and 31 Cyg (a similar composite).

I have measured positions of all the features strong enough to be emission lines by plotting the spectrum in 10–20 Å segments on a computer terminal and bisecting the line with a cursor. For strong lines, I fit a Gaussian to the profile and used its fitted center as the observed wavelength. I then identified the transitions with the help of the ultraviolet multiplet tables (Moore 1950–1970), augmented by Kurucz's (1981) calculated spectrum of Fe II. Measured wavelengths, fluxes, identifications, and laboratory wavelengths of all these features are given in Table 1, and their positions are plotted in Figure 1. The fluxes represent the emission in the line above the continuum longward of 2810 Å and the emission above zero intensity shortward of 2810 Å, in units 10^{-14} ergs cm^{-2}s^{-1}. Most of the identified lines are included in Moore's ultraviolet multiplet tables. However, these tables are incomplete below 2000 Å, and I have identified the missing Fe II lines from Kurucz's lists, giving the excitation potential of the lower level in eV and designating the levels of the transition with the same symbols used in the UV multiplet tables, when possible. I denote unclassified upper levels with a "?".

Lines that were saturated in the *IUE* spectra are noted with an "s" in the notes column of Table 1; those affected by a reseau, by an "r"; and those that might be affected by the edge of an echelle order, by an "o". Some previous identifications of emission lines in other ζ Aur binaries were published by Stencel & Chapman (1981) and by Bauer & Stencel (1989). Those lists addressed only the stronger lines, and, while most of the identifications are the same as ours, there are some exceptions. Specifically, Stencel & Chapman identify the line at 1640.22 Å as He I and the line at 2790.92 as Mg II UV3. In the notes to Table 1, I identify those lines that are also clearly present in the eclipse spectrum of ζ Aur with a "Z", those identified in ζ Aur by Stencel & Chapman with an "S", those present in the eclipse

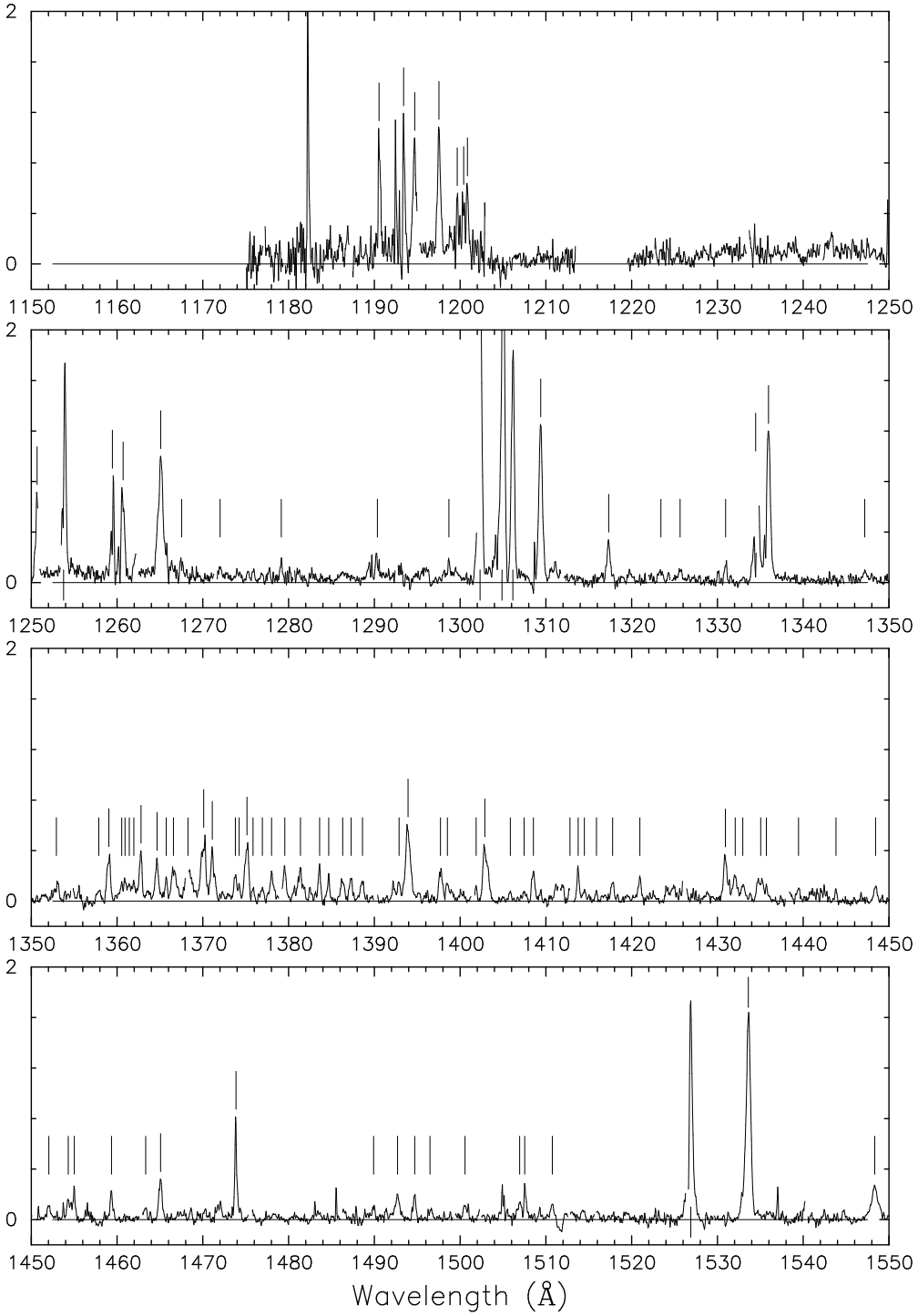

Figure 1a: The spectrum of 32 Cyg in total eclipse. Features listed in Table 1 are marked with the vertical lines above or below the spectrum. The vertical scale is 10^{-11} ergs cm^{-2}s^{-1}Å^{-1}, and is based on calibrations given by Bohlin & Holm (1980), Cassatella & Harris (1983), and Cassatella et al. (1983). I have omitted wavelengths affected by camera reseaux.

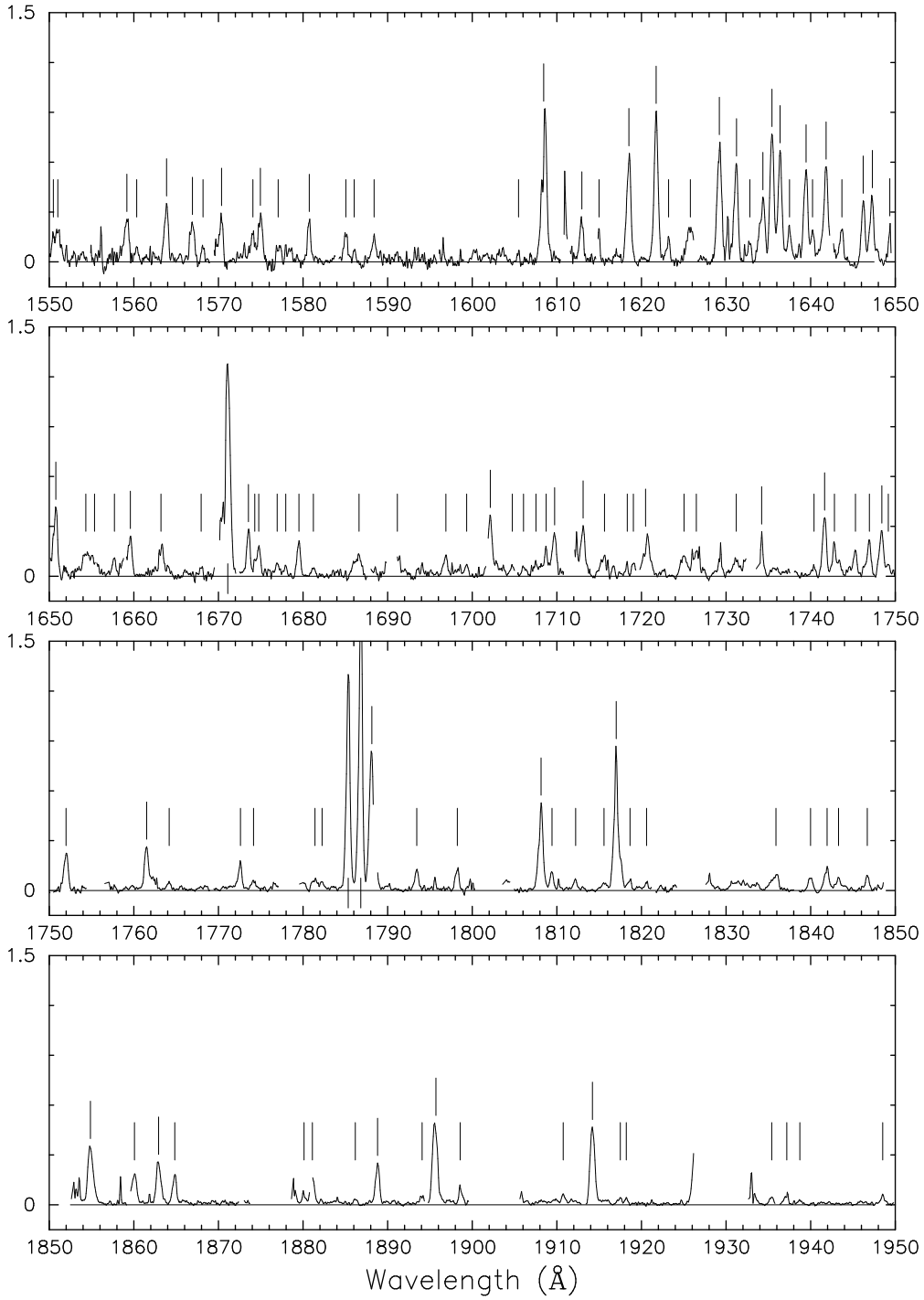

Figure 1b: The spectrum of 32 Cyg in total eclipse, continued.

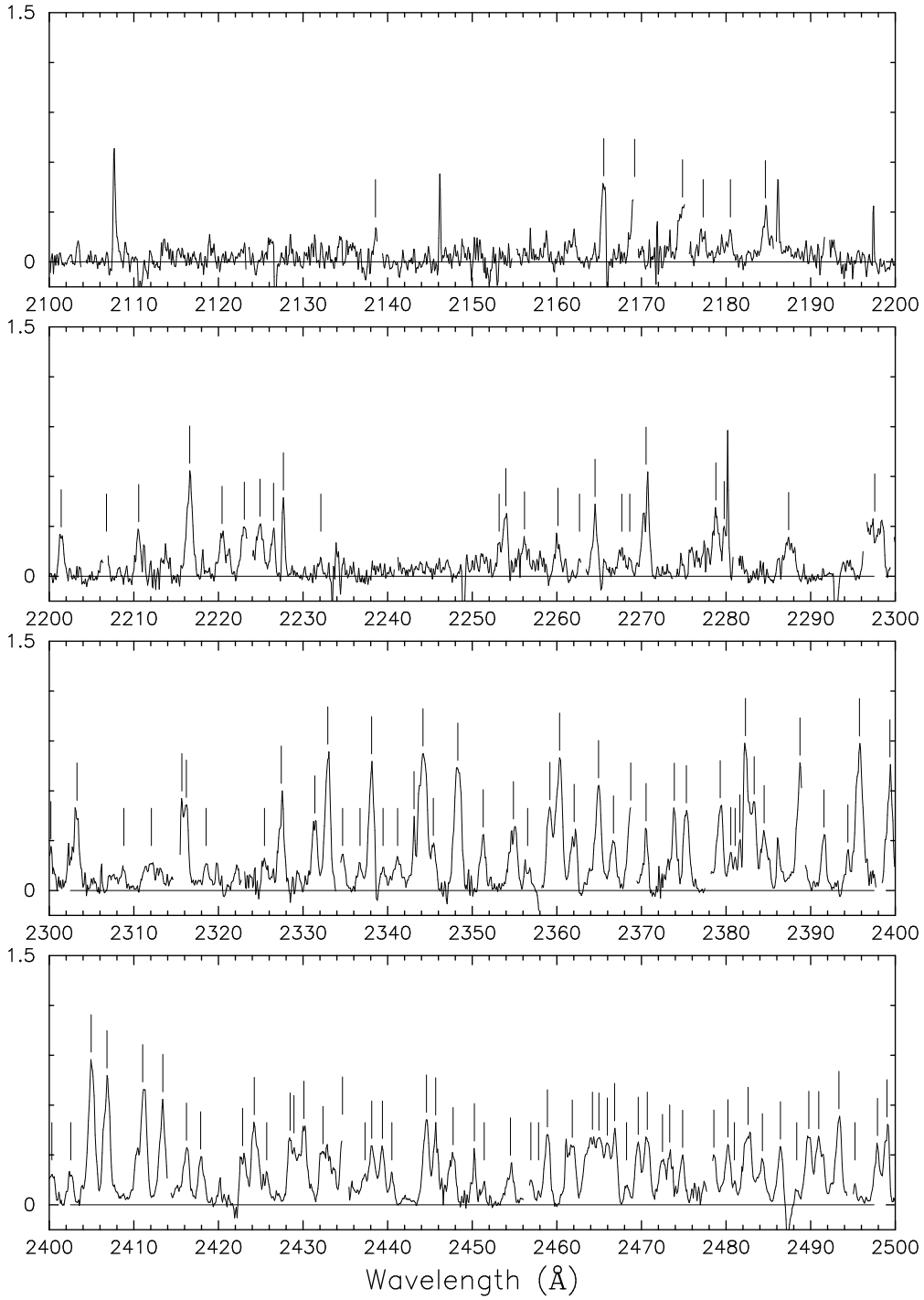

Figure 1c: The spectrum of 32 Cyg in total eclipse, continued.

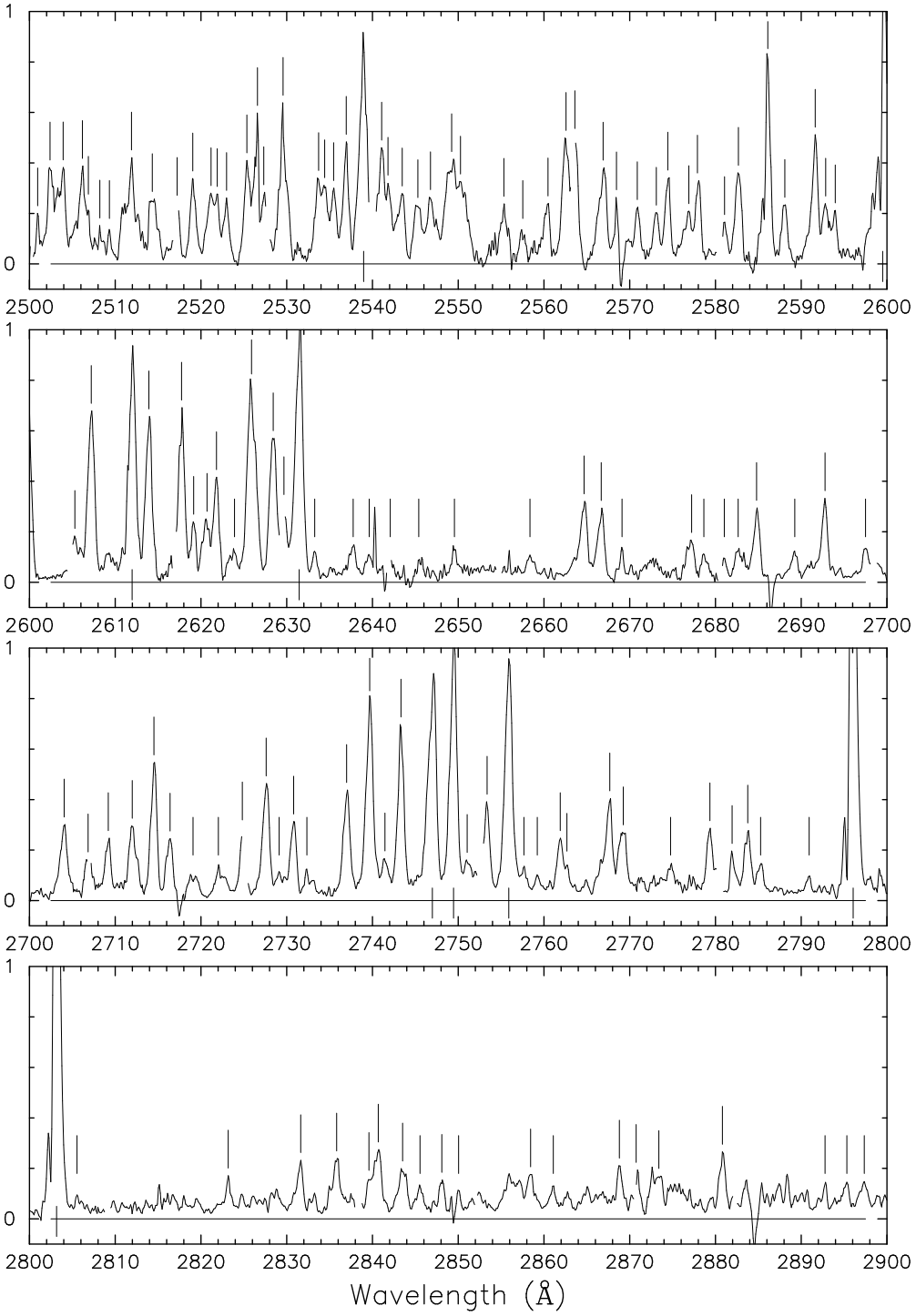

Figure 1d: The spectrum of 32 Cyg in total eclipse, continued.

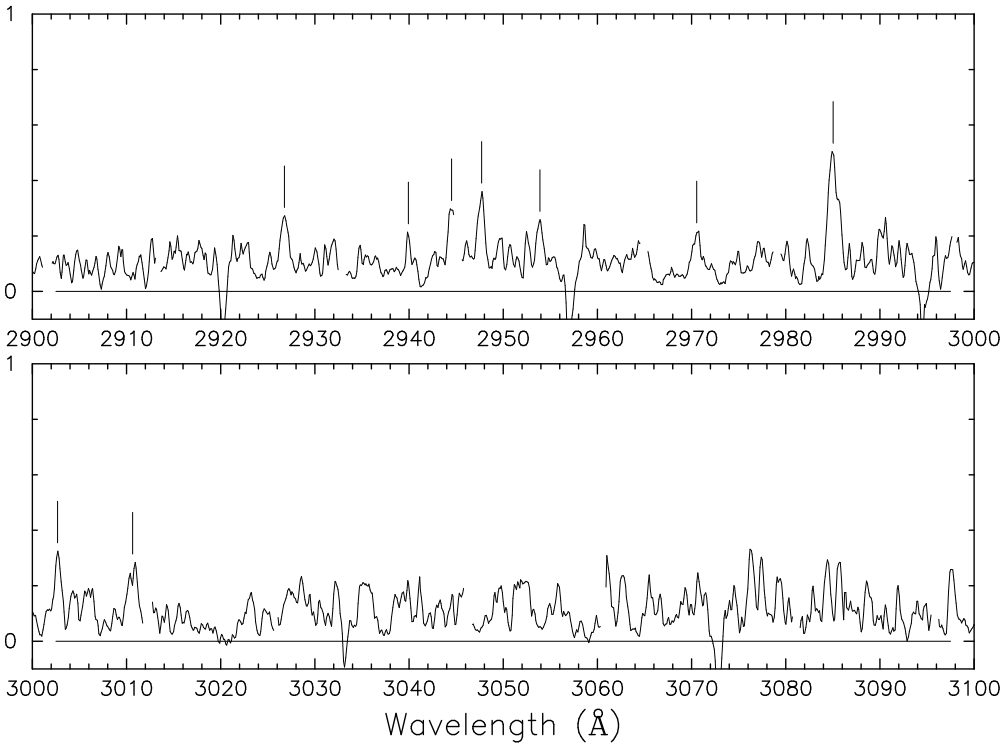

Figure 1e: The spectrum of 32 Cyg in total eclipse, concluded.

spectrum of 31 Cyg with a "3", and those noted in 31 Cyg by Bauer & Stencel with a "B".

Measurements of interstellar absorption features superimposed on the emission lines give a velocity of -18.8 km s^{-1} for the short-wavelength spectrum (6 lines of Si II, S II, and Fe II) and -20.6 km s^{-1} for the long-wavelength spectrum (6 lines of Fe II and Mg II). These two values agree to within their errors of measurement, ± 2 km s^{-1}. I have therefore not applied any corrections to the measured wavelengths.

The identifications in Table 1 for the most part are based on Moore's *Ultraviolet Multiplet Tables* and on Kurucz's predicted wavelengths for those Fe II lines not in *Moore*, which are all rather old references. I have chosen to do this because Moore's tables give a comprehensive framework of the multiplets for identifying the lines and associating them with atomic structure, hence excitation. Somewhat newer values of the wavelengths are available from Morton (2003) and NIST (2008), particularly for the lower-lying multiplets, but there does not seem to be a recent comprehensive compilation of the UV wavelengths sorted into multiplets. The most recent wavelengths from Kurucz (2008) seem to contain only trivial differences from Kurucz (1981) for the lines considered.

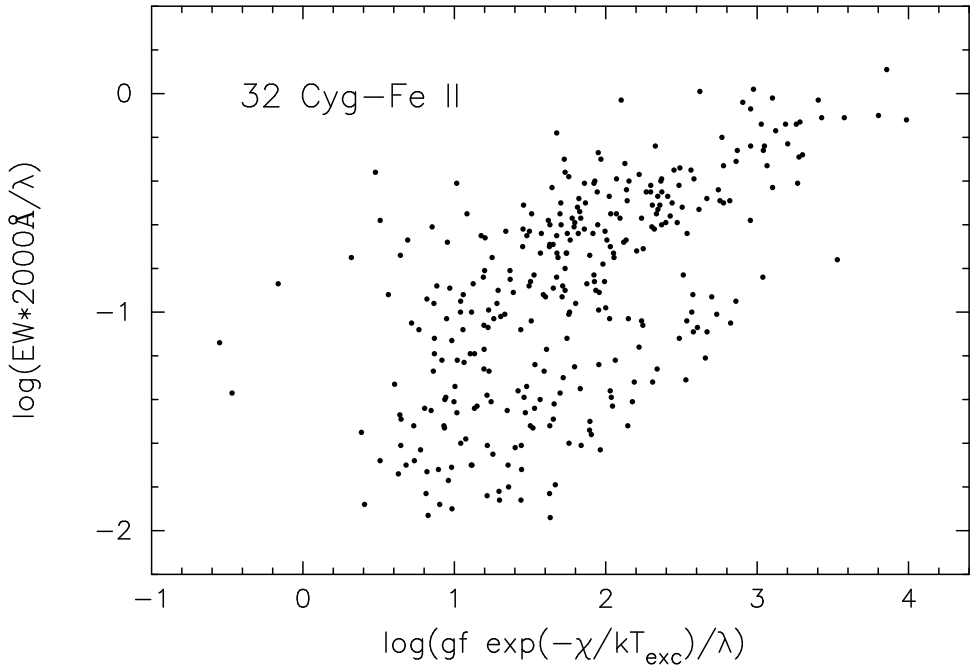

Figure 2: A curve of growth for the Fe II emission lines in 32 Cyg. Equivalent widths are with respect to a smoothed low-dispersion spectrum obtained far from eclipse (SWP10922 & LWR9604), and the intrinsic line strengths are based on Kurucz's (1981) theoretical f values. This calculation assumes the excitation temperature is 10,000 K, but the result is roughly the same for temperatures beteween 5000 K and 20,000 K.

3 Nature of the Spectrum

Table 1 contains 489 features, the strongest of which are intrinsically strong lines of common ions. Atomic spectra definitely identified are Fe II, Si II, S II, C II, Ni II, Mg II, Cr II, O I, N I, Al II, Al III, Fe III, Si IV, and C IV. Furthermore, *IUE may* have detected radiation scattered by the wings of H I Lyα (see the top panel in Figure 1a). The spectra Fe II, Si II, Ni II, and Cr II are identified clearly by numerous lines of multiplets from low lying levels. O I, Al III, Fe III, Si IV, and C IV are represented by only one multiplet each in this wavelength range, but it is strong enough to be unambiguously identified. N I and Al II both have few lines but more than one multiplet. Only 8 % of the features remain unidentified, and most of these are weak lines that were not clearly in the spectrum of ζ Aur.

Seventy-four percent of the lines can be identified as Fe II. Almost all of the lines are intrinsically stronger than $gf = 10^{-2}$ (with gf from Kurucz 1981). Figure 2 is a curve of growth showing the distribution of the strengths these Fe II lines with intrinsic strength. Although curves of growth have been used extensively to analyze the shell *absorption* lines in these stars, the large scatter for these *emission* lines means a curve of growth for the *global* absorption is meaningless. Most of the lines to the bottom right of this diagram are from relatively low lying multiplets that are seen in the photospheric spectrum of the B star. So

some of their weakness is caused calculating the equivalent width with respect to the local continuum, not the level of the photospheric line. However, this should be of the order of only a factor of two. Scatter to the top left in the diagram comes from highly excited relatively intrinsically weak lines, which means that there is significant redistribution from stronger lines originating at low excitation potential to others with higher excitational potentials. The emission-line spectrum of 32 Cyg, as expected, is formed in an optically thick shell in which fluorescent processes are important.

4 Discussion

From the standpoint of chromospheric structure, the most important lines are those excited in the chromosphere itself and not merely scattered from the spectrum of the B star. There are very few such lines (Eaton 1992). The best seems to be Al II] λ2669, which is fortuitously isolated in the spectra of these binaries. Others are the fluorescent lines of Fe I UV44, which are formed by scattering Mg II UV1 deep in the chromosphere (Harper 1990). Those two Fe lines are detected in the ζ Aur binaries, but the longer one is too severely blended with wind-scattered lines for us to analyze them properly. The density-sensitive C II] UV0.1 multiplet ought to be present (Schröder et al. 1988), but these lines are too weak to detect, even in this well-exposed *IUE* spectrum of 32 Cyg (see Fig. 1c), although Harper et al. (2005) recorded the strongest component of it in ζ Aur with *HST*.

Winds from giant stars in binaries with hot companions must differ somewhat from winds of single stars. A cavity is ionized in the wind around the B star, and its consequence is to eliminate all the wind lines of singly ionized metals at low velocities. Thus we do not see Fe II absorptions from the gas between the two stars flowing toward the B star. Yet, we know this gas exists because of its accretion onto the B star (e.g., Ahmad & Stencel 1988). Furthermore, it is revealed by the strong lines of Al III and Fe III with their velocities preponderantly toward the hot star (Eaton & Bell 1994; § 3.6 for 31 Cyg). Che et al. (1983) have argued that the ionization occurs only in the B star's H II region, where the ground states of neutral oxygen and nitrogen and the first ions of Fe, Mg, Si, S, etc. are shielded from ionizing radiation. An ionized cavity may extend beyond the H II region since the Balmer continuum of a B star will ionize most metals from excited metastable states. Further, this cavity can exist for an ion like Mg II without metastable levels, even in systems having late B star, for unless the electron density is high enough, the B star's continuum will excite enough Mg ions into their second level for the majority of them to get ionized (Eaton et al. 1990). Once the ion is ionized, it must recombine, and this is often long in comparison to the star's orbital period (Che et al.). Thus spectra like S II, formed by ions that recombine rapidly, should be stronger in the wind than expected for cosmic abundances.

Acknowledgements

This work was part of a student research project by Deena Rembert, a Tennessee State undergraduate, whose help I gratefully acknowledge. I also thank A. M. Heiser for help with

several references. I am grateful to NASA for supporting this research through grants NAG 5-599 and NAG 5-1372 and to the State of Tennessee for general support of the program in automated astronomy at TSU.

List of data Tables

1. Emission Lines of 32 Cygni in Total Eclipse [TABLE1]

References

Ahmad, I. A., Stencel, R. E., 1988, ApJ, 329, 797

Baade, R., Kirsch, T., Reimers, D., Toussaint, F., Bennett, P. D., Brown, A., Harper, G.M., 1996, ApJ, 466, 979

Bauer, W. H., Stencel, R. E., 1989, ApJS, 69, 667

Bauer, W. H., Gull, T. R., Bennett, P. D. 2008, AJ, 136, 1312

Bohlin, R. C., Holm, A. V., 1980, NASA IUE Newsletter, No. 10, p. 37

Cassatella, A., Harris, A. W., 1983, NASA IUE Newsletter, No. 23, p. 21

Cassatella, A., Ponz, D., Selvelli, P. L., 1983, NASA IUE Newsletter, No. 21, p. 46

Chapman, R. D., 1981, ApJ, 248, 1043

Che, A., Hempe, K., Reimers, D., 1983, A&A, 126, 225

Eaton, J. A., 1992, MNRAS, 258, 473

Eaton, J. A., 1993, AJ, 105, 1525

Eaton, J. A., Henry, G. W., Odell, A. P. 2008, ApJ, 679, 1490

Eaton, J. A., Bell, C., 1994, AJ, 108, 2276

Eaton, J. A., McCluskey, G. E., Kondo, Y., Shore, S. N., 1990, AJ, 100, 799

Harper, G. M., 1990, MNRAS, 243, 381

Harper, G. M., Brown, A., Bennett, P. D., Baade, R., Walder, R., Hummel, C. A., 2005, AJ, 129, 1018

Judge, P. G., 1986, MNRAS, 223, 239

Judge, P. G., Jordan, C., 1991, ApJS, 77, 75

Judge, P. G., Jordan, C., Feldman, U., 1992, ApJ, 384, 613

Kurucz, R. L., 1981, "Semiempirical Calculation of gf Values, IV: Fe II," SAO Spec. Rept., No. 390

Kurucz, R. L., 2008, "Kurucz atomic line database," http://kurucz.harvard.edu/ and http://cfa-www.harvard.edu/amp/tools.html

McClintock, W., Gerola, H., Linsky, J. L., Henry, R. C., Moos, H. W., 1975, ApJ, 202, 165

Moore, C. E., 1950, "An ultraviolet multiplet table," NBS Circ., No. 488, Sect. 1 (H–V)

Moore, C. E., 1952, "An ultraviolet multiplet table," NBS Circ., No. 488, Sect. 2 (Cr–Nb)

Moore, C. E., 1962, NBS Circ., No. 488, Sect. 4

Moore, C. E., 1965, "Selected Tables of Atomic Spectra," NSRDS–NBS 3, Sect. 1 (Si II–Si IV)

Moore, C. E., 1970, "Selected Tables of Atomic Spectra," NSRDS–NBS 3, Sect. 3 (C I–C IV)

Morton, D. C., 2003, ApJS, 149, 205

NIST (U.S. National Institute of Standards and Technology), 2008, "NIST Atomic Spectra Database," http://physics.nist.gov/PhysRefData/ASD/index.html

Schröder, K.-P., Reimers, D., Carpenter, K. G., Brown, A., 1988, A&A, 202, 142

Stencel, R. E., Chapman, R. D., 1981, ApJ, 251, 597

Wilson, O. C., Abt, H. A., 1954, ApJS, 1, 1

Wright, K. O., 1970, Vistas in Astr., 12, 147

Table 1: Emission Lines of 32 Cygni in Total Eclipse (page 1).

λ_{obs}	Flux	λ_{lab}	Identification	Notes	λ_{obs}	Flux	λ_{lab}	Identification	Notes
1190.54	329	1190.418	Si II UV5	Z3B	1368.26	193	1368.262	Fe II (3.39,a^2F-?^{2}D^o)	rZ
1193.41	324	1193.284	Si II UV5	Z3B			1368.094	Fe II (1.70,a^4P-v^{4}D^o)	
1194.70	463	1194.496	Si II UV5	rZ3B	1370.10	313	1370.200	Ni II UV8	Z3
1197.53	496	1197.389	Si II UV5	Z3B	1371.10	209	1371.022	Fe II (2.63,a^4H-?^{4}G^o)	oZ
1199.66	186	1199.550	N I UV1		1373.79	80	1373.718	Fe II (3.72,b^2G-?^{2}F^o)	Z
1200.41	179	1200.218	N I UV1	Z	1374.24	38	1374.14	Ni II UV9	Z
1200.85	207	1200.707	N I UV1	Z	1375.15	241	1375.173	Fe II (2.66,a^4H-?^{4}G^o)	Z
1250.68	272	1250.500	S II UV1	rZ3B	1375.85	35			Z
1253.76	587	1253.790	S II UV1	Z3B	1376.94	42			Z
1259.46	250	1259.53	S II UV1	ZS3B	1378.02	106	1377.987	Fe II (3.81,b^2G-?^{2}F^o)	Z
1260.71	323	1260.418	Si II UV4	ZS3B	1379.56	131	1379.470	Fe II (2.68,a^4H-?^{4}G^o)	rZ
		1260.540	Fe II UV9		1381.38	119	1381.36	Ni II UV8	Z
1265.09	702	1264.730	Si II UV4	ZS3B	1383.62	90	1383.580	Fe II (2.69,a^4H-?^{4}G^o)	Z
		1265.023	Si II UV4		1384.67	71			oZ
1267.53	88	1267.437	Fe II UV9		1386.31	89	1386.182	Fe II (3.25,a^4G-?^{4}F^o)	Z
1272.01	62	1272.001	Fe II UV9	r	1387.29	71	1387.219	Fe II (2.52,a^2H-?^{4}F^o)	Z
1279.14	65	1279.101	Fe II (3.20,b^2P-?^{2}S^o)		1388.62	73	1388.597	Fe II (3.42,a^2F-?^{2}G^o)	Z
1290.36	74	1290.204	Fe II UV88?		1392.88	56	1392.817	Fe II (2.58,a^2H-?^{2}G^o)	Z
1298.69	55	1298.815	Fe II UV87?	Z	1393.92	405	1393.755	Si IV UV1	ZS3B
1302.32	1287	1302.174	O I UV2	rZS3B	1397.71	127	1397.572	Fe II (2.81,b^4F-?^{4}G^o)	
1304.88	1420	1304.860	O I UV2	ZS3B			1397.845	Fe II (3.20,b^2P-?^{2}P^o)	
		1304.369	Si II UV3		1398.51	65			o
1306.15	789	1306.023	O I UV3	ZS3B	1401.87	35	1401.774	Fe II (2.83,b^4F-?^{4}G^o)	r
1309.39	658	1309.274	Si II UV3	ZS3B	1402.88	295	1402.730	Si IV UV1	ZS3B
1317.32	161	1317.38	Ni II UV10	Z3	1405.85	24	1405.800	Fe II (2.84,b^4F-?^{4}G^o)	
1323.41	58				1407.46	24	1407.483	Fe II (2.84,b^4F-?^{4}G^o)	Z
1325.64	45				1408.55	102	1408.474	Fe II (2.63,a^4H-?^{4}H^o)	Z
1330.96	55	1330.952	Fe II (3.39,a^2F-?^{2}D^o)	o	1412.81	31	1412.834	Fe II UV47	r
1334.45	119	1334.532	C II UV1	rZS3B	1413.76	85	1413.702	Fe II (2.66,a^4H-?^{4}H^o)	Z
1335.96	657	1335.663	C II UV1	ZS3B	1414.49	37	1414.402	Mn II UV78?	Z
		1335.708	C II UV1		1415.89	22	1415.755	Mn II UV88?	Z
1347.18	55	1347.2	Cl I UV2?		1417.78	64	1417.773	Fe II (2.68,a^4H-?^{4}H^o)	Z
1352.92	35				1420.96	78	1420.912	Fe II (2.69,a^4H-?^{4}H^o)	Z
1357.87	46	1357.796	Fe II (4.08,a^2I-?^{2}K^o)	oZ	1430.92	169	1430.893	Fe II (3.27,b^2H-?^{2}H^o)	Z
1359.05	174	1358.937	Fe II (3.24,b^2H-?^{2}G^o)	Z			1430.781	Fe II (3.24,b^2H-?^{2}H^o)	
		1358.764	Cu II UV3?		1432.08	105			
1360.55	37	1360.450	Fe II (4.14,c^2G-?^{2}H^o)		1432.95	66	1432.875	Fe II (2.81,b^4F-?^{4}F^o)	
1360.92	59	1360.858	Fe II (3.24,b^2H-?^{2}G^o)		1435.05	143			
1361.43	47	1361.373	Fe II (1.67,a^4P-v^{4}D^o)		1435.71	44			
		1361.366	Fe II (3.27,b^2H-?^{2}G^o)		1439.46	43			
1361.95	57				1443.83	26	1443.737	Fe II (3.77,b^2G-?^{2}G^o)	
1362.79	145	1362.771	Fe II UV152	Z	1448.44	52	1448.393	Fe II (3.39,a^2F-?^{2}F^o)	Z
1364.66	158	1364.578	Fe II (3.27,b^2H-?^{2}G^o)	Z			1448.354	Fe II (3.81,b^2G-?^{2}G^o)	Z
1365.73	56	1365.678	Fe II (4.15,c^2G-?^{2}H^o)	Z	1452.04	46	1451.989	Fe II (3.81,b^2G-?^{2}G^o)	Z
1366.57	164	1366.394	Fe II (2.83,b^4F-?^{4}D^o)	Z	1454.31	41	1454.311	Fe II (3.15,a^4G-?^{4}G^o)	Z

Table 1: Emission Lines of 32 Cygni in Total Eclipse (page 2).

λ_{obs}	Flux	λ_{lab}	Identification	Notes	λ_{obs}	Flux	λ_{lab}	Identification	Notes
1455.01	72	1454.96	Ni II UV7	Z	1631.24	350	1631.124	Fe II UV8	Z
1459.35	77	1459.311	Fe II UV193	Z			1631.110	Fe II (0.39,a^4F-z^2F^o)	
1463.34	40	1463.204	Fe II (3.20,a^4G-?$^4G^o$)	r	1632.81	57	1632.672	Fe II UV43	
1465.08	152	1465.043	Fe II UV193	Z	1634.35	284	1634.353	Fe II UV8	Z3
1473.87	230	1473.834	Fe II UV193	Z			1633.907	Fe II UV43	
1489.91	36				1635.43	454	1635.389	Fe II UV68	ZS3
1492.71	109	1492.630	N I UV4		1636.38	352	1636.334	Fe II UV8	ZS3
1494.70	78	1494.669	N I UV4		1637.50	108	1637.400	Fe II UV42	Z
1496.48	31	1496.526	Fe II (3.15,a^4G-?$^4H^o$)		1639.46	326	1639.403	Fe II UV8	ZS3
1500.57	53	1500.44	Ni II UV7		1640.22	87	1640.167	Fe II UV43	ZS
1506.94	60	1506.903	Fe II (3.20,a^4G-?$^4H^o$)	Z	1641.83	436	1641.761	Fe II UV68	rZS3
		1506.536	Fe II (4.48,b^2D-?$^2D^o$)		1643.69	112	1643.588	Fe II UV42	Z
1507.53	93		noise?		1646.20	191	1646.187	Fe II UV68	ZS3
1510.75	54	1510.86	Ni II UV6		1647.29	227	1647.161	Fe II UV68	Z3
1526.90	864	1526.719	Si II UV2	rZS3B	1649.35	61	1649.583	Fe II UV68	o
		1526.536	Fe II (2.28,a^2P-v^2D^o)				1649.444	Fe II UV42	
1533.61	1121	1533.445	Si II UV2	ZS3B	1650.78	232	1650.709	Fe II UV68	Z
1548.34	245	1548.195	C IV UV1	ZS3B	1654.32	128	1654.105	Fe II UV68	Z
1550.48	64	1550.260	Fe II UV45				1654.484	Fe II UV42	
1551.01	103	1550.768	C IV UV1	ZS3B	1655.36	91	1655.042	Fe II UV68	Z
1559.18	170	1559.106	Fe II UV45	Z			1655.506	Fe II (3.94,b^2F-u^2D^o)	
1560.34	44	1560.252	Fe II UV45		1657.70	58	1657.545	Fe II (2.28,a^2P-w^2D^o)	
1563.87	191	1563.790	Fe II UV45	Z3	1659.59	148	1659.487	Fe II UV40	Z
1566.92	145	1566.825	Fe II UV44	Z3	1663.21	119	1663.226	Fe II UV40	Z
1568.18	39	1568.031	Fe II UV45		1667.95	23	1667.913	Fe II (2.39,a^2P-w^2P^o)	
1570.37	129	1570.248	Fe II UV45	Z	1671.11	848	1670.81	Al II UV2	oZ3B
1574.08	69	1574.038	Fe II (2.52,a^2H-w^2G^o)	Z			1670.759	Fe II UV40	
		1573.831	Fe II UV45		1673.55	142	1673.470	Fe II UV102	Z
1574.96	159	1574.931	Fe II UV45	oZ3	1674.29	43	1674.258	Fe II UV41	
		1574.778	Fe II UV44		1674.77	72	1674.716	Fe II UV40	Z
1577.06	59	1577.158	Fe II UV45		1676.94	38	1676.871	Fe II UV41	Z
1580.73	121	1580.635	Fe II UV44	Z	1677.95	23	1677.842	Fe II (2.34,a^2P-w^2D^o)	Z
1585.06	91	1584.954	Fe II UV44	Z	1679.52	104	1679.388	Fe II UV102	Z
1586.05	26	1585.999	Fe II (2.64,a^2D-v^2D^o)		1681.22	25	1681.111	Fe II (0.35,a^4F-z^2G^o)	
1588.40	85	1588.295	Fe II UV44	Z	1686.62	64	1686.457	Fe II UV40	Z
1605.47	19	1605.324	Fe II (1.96,a^2G-v^2F^o)		1691.15	108	1691.289	Fe II UV41	oZ
1608.44	597	1608.446	Fe II UV8	Z3	1696.88	77	1696.800	Fe II UV38	Z
1612.95	141	1612.814	Fe II UV43	Z	1699.34	37	1699.199	Fe II UV85	
1614.98	65			r	1702.13	249	1702.045	Fe II UV38	rZ3
1618.51	389	1618.464	Fe II UV8	Z3			1701.952	Fe II UV85	
1621.73	522	1621.685	Fe II UV8	Z3	1704.74	41	1704.643	Fe II UV39	
1623.20	70	1623.102	Fe II UV43		1706.06	34	1706.179	Fe II UV38?	
1625.78	189	1625.525	Fe II UV43	rZ	1707.53	31	1707.411	Fe II UV84	Z
1629.21	451	1629.155	Fe II UV8	Z3			1707.669	Fe II (0.30,a^4F-z^4H^o)	
		1629.371	Fe II (2.03,a^2G-v^2F^o)		1708.74	44	1708.627	Fe II UV38	Z

Table 1: Emission Lines of 32 Cygni in Total Eclipse (page 3).

λ_{obs}	Flux	λ_{lab}	Identification	Notes	λ_{obs}	Flux	λ_{lab}	Identification	Notes
1709.73	149	1709.678	Fe II UV84	Z	1820.61	25			Z
		1709.560	Fe II UV37		1835.89	95	1835.869	Fe II UV98	Z
		1709.600	Ni II UV4		1839.98	50			Z
1713.11	182	1713.002	Fe II UV38	Z	1841.94	97	1841.701	Fe II UV65	Z
1715.63	41	1715.507	Fe II UV84	Z	1843.30	52			Z
1718.32	28	1718.123	Fe II UV38	Z	1846.69	47	1846.581	Fe II UV98	Z
1719.05	39	1718.984	Fe II (2.54,a^2D-w^2D^o)	rZ	1854.87	283	1854.722	Al III UV1	ZS3B
1720.48	205	1720.621	Fe II UV38	Z3	1860.08	140	1860.040	Fe II UV97	rZ3
		1720.042	Fe II UV84				1859.744	Fe II UV65	
1725.03	79	1724.963	Fe II UV37	Z	1862.92	180	1862.782	Al III UV1	ZS3B
		1724.847	Fe II UV39?		1864.84	109	1864.656	Fe II UV126	Z3
1726.49	91	1726.394	Fe II UV38	Z3			1864.743	Fe II UV126	
		1726.056	Fe II (2.64,a^2D-w^2P^o)		1880.12	33	1880.046	Fe II UV141	Z
1731.20	69	1731.038	Fe II UV110	Z	1881.10	100	1880.976	Fe II UV126	rZ
	.	1731.336	Fe II (1.96,a^2G-w^2H^o)				1881.180	Ni II UV24?	
1734.21	103		noise?		1886.17	19	1886.06	Ni II UV23?	
1740.40	31		noise?		1888.81	145	1888.729	Fe II UV125	Z3
1741.64	202	1741.560	Ni II UV5	Z3	1894.07	29	1894.006	Fe II UV125	Z
1742.81	123	1742.709	Fe II (2.03,a^2G-w^2H^o)	Z3	1895.71	373	1895.456	Fe III UV34	ZS3B
		1742.734	N I UV9				1895.675	Fe II UV124	
1745.29	79	1745.242	Fe II UV101	Z3	1898.58	59	1898.538	Fe II UV140	Z
		1745.246	N I UV9		1910.75	37	1910.669	Fe II UV124	Z3
1746.94	137	1746.816	Fe II UV101	Z3	1914.20	321	1914.056	Fe III UV34	Z3B
1748.41	181	1748.30	Ni II UV5	Z3	1917.50	26	1917.337	Fe II UV96	
1749.18	24	1749.123	Fe II (1.96,a^2G-x^2F^o)	Z	1918.20	18	1918.114	Fe II UV138	
1751.99	141	1751.92	Ni II UV4	Z3	1935.40	28	1935.296	Fe II UV96	Z
1761.52	179	1761.379	Fe II UV101	Z3	1937.18	40	1936.781	Fe II UV96	Z
1764.18	27	1764.119	Fe II (2.03,a^2G-x^2F^o)	Z	1938.72	17		noise?	
1772.60	90	1772.518	Fe II UV99	Z	1948.51	34	1948.372	Fe II UV123	Z
1774.14	43	1773.96	Ni II UV3	Z	2138.56	140	2138.60	Ni II UV13	r
1781.41	53	1781.343	Fe II (2.28,a^2P-x^2D^o)		2165.55	282	2165.55	Ni II UV13	ZS3
1782.25	36				2169.19	271	2169.10	Ni II UV13	rZ3
1785.34	698	1785.262	Fe II UV191	sZS3B	2174.85	355	2175.16	Ni II UV13	rZ3
1786.82	917	1786.739	Fe II UV191	sZS3B	2177.30	138	2177.025	Fe II UV106?	
1788.13	634	1787.997	Fe II UV191	rZS3B	2180.52	122			
		1788.50	Ni II UV5		2184.65	220	2184.61	Ni II UV13	Z3
1793.44	73	1793.371	Fe II UV99	Z	2201.41	175	2201.41	Ni II UV13	Z3
1798.23	71	1798.163	Fe II UV142	Z			2201.595	Fe II UV367	
1808.13	323	1808.003	Si II UV1	ZS3B	2206.76	126	2206.71	Ni II UV13	rZ3
1809.42	58	1809.316	Fe II UV142	Z	2210.57	166	2210.38	Ni II UV13	Z
1812.22	37	1812.07	Ni II UV24	Z			2210.952	Fe II UV118	
1815.57	33	1815.410	Fe II (2.54,a^2D-w^2F^o)	Z	2216.61	507	2216.479	Ni II UV12	ZS3
1817.01	517	1816.921	Si II UV1	sZS3B	2220.43	202	2220.388	Fe II UV118	Z3
		1817.420	Si II UV1		2223.06	364	2222.948	Ni II UV12	rZS3
1818.65	37	1818.509	Fe II UV66	Z	2224.91	295	2224.88	Ni II UV12	ZS3

Table 1: Emission Lines of 32 Cygni in Total Eclipse (page 4).

λ_{obs}	Flux	λ_{lab}	Identification	Notes	λ_{obs}	Flux	λ_{lab}	Identification	Notes
2226.52	178	2226.34	Ni II UV12	ZS3	2345.39	173	2345.327	Fe II UV165	Z3
2227.67	172	2227.407	Fe II UV168	Z			2345.44	Ni II UV11?	
		2227.469	Fe II UV369		2348.30	772	2348.300	Fe II UV3	Z3
2232.11	53	2232.073	Fe II (2.03,a^2G-z^4H^o)				2348.118	Fe II UV36	
2253.17	99	2253.119	Fe II UV4	3	2351.30	239	2351.198	Fe II UV165	Z3
2253.97	261	2253.856	Ni II UV12	Z3	2354.87	435	2354.884	Fe II UV35	Z3
2256.18	210	2255.979	Fe II UV34	Z	2356.55	125	2356.41	Ni II UV22	Z3
2260.13	176	2260.228	Fe II UV5	Z3	2359.17	368	2359.111	Fe II UV3	Z3
		2260.078	Fe II UV4		2360.32	732	2360.287	Fe II UV36	Z3
2262.68	77	2262.686	Fe II UV5	r	2362.04	325	2362.014	Fe II UV35	Z3
2264.51	250	2264.456	Ni II UV12	ZS3	2364.92	557	2364.825	Fe II UV3	Z3
		2264.589	Fe II UV246?		2366.69	271	2366.864	Fe II UV2	Z3
2267.68	159	2267.584	Fe II UV4	Z			2366.591	Fe II UV35	
2268.62	48	2268.562	Fe II UV5	Z	2368.74	429	2368.593	Fe II UV36	rZ3
2270.55	480	2270.209	Ni II UV12	ZS3	2370.54	237	2370.494	Fe II UV35	Z3
2278.80	352	2278.771	Ni II UV22	Z3	2373.88	312	2373.733	Fe II UV2	Z3
2279.78	133	2279.918	Fe II UV4	Z3	2375.31	410	2375.192	Fe II UV36	Z3
2287.40	268	2287.082	Ni II UV22	Z3			2375.426	Ni II UV21?	
2297.58	706	2296.662	Fe II UV167?	rZ3	2379.31	477	2379.275	Fe II UV36	Z3
		2296.769	Fe II UV133				2379.155	Fe II UV211	
		2297.140	Ni II UV11				2379.003	Fe II UV182	
		2297.486	Ni II UV11		2380.56	116			3
		2298.225	Fe II UV133		2381.08	99	2380.757	Fe II UV3?	Z3
		2298.269	Ni II UV21		2381.63	146			Z3
2300.19	234	2300.10	Ni II UV27?	Z	2382.29	639	2382.034	Fe II UV2	ZS3
2303.28	504	2302.98	Ni II UV11	Z3	2383.32	349	2383.060	Fe II UV2	Z3
2308.83	86			Z3			2383.242	Fe II UV36	
2312.08	127	2312.028	Fe II UV105	Z	2384.50	311	2384.386	Fe II UV36	Z3
2315.68	230		noise?	Z3	2388.74	741	2388.629	Fe II UV2	rZS3
2316.20	277	2316.034	Ni II UV11	Z3	2391.57	424	2391.475	Fe II UV35	Z3
2318.55	126	2318.343	Fe II UV183?	Z	2394.40	135	2394.518	Ni II UV20?	Z3
2325.44	146	2325.296	Fe II UV183?	Z	2395.76	903	2395.627	Fe II UV2	Z3
2327.43	409	2327.391	Fe II UV3	Z3			2395.416	Fe II UV2	
		2327.953	Fe II UV183?		2399.37	441	2399.237	Fe II UV2	Z3
2331.39	308	2331.308	Fe II UV35	Z3			2399.237	Fe II UV36	
2332.93	661	2332.798	Fe II UV3	Z3	2400.31	158	2400.338	Fe II UV244	Z3
2334.67	155	2334.590	Ni II UV20?	rZ3			2400.274	Fe II UV181	
2336.74	110	2336.59	Ni II UV27?	Z	2402.55	158	2402.597	Fe II UV36	Z3
2338.10	554	2338.005	Fe II UV3	Z3	2404.96	816	2404.882	Fe II UV2	Z3
2339.46	95	2339.408	Fe II UV105	Z	2406.82	743	2406.660	Fe II UV2	Z3
2341.18	181			Z3	2411.05	733	2411.062	Fe II UV2	Z3
2343.12	200	2343.495	Fe II UV3	Z3			2410.521	Fe II UV2	
2344.18	953	2344.278	Fe II UV3	Z3	2413.42	486	2413.308	Fe II UV2	Z3
		2343.958	Fe II UV35		2416.22	309	2416.134	Ni II UV20?	Z3
					2417.90	230	2417.859	Fe II UV244	Z3

Table 1: Emission Lines of 32 Cygni in Total Eclipse (page 5).

λ_{obs}	Flux	λ_{lab}	Identification	Notes	λ_{obs}	Flux	λ_{lab}	Identification	Notes
2422.86	265	2422.688	Fe II UV301?	Z3	2473.34	183	2473.314	Fe II UV148	Z3
2424.24	445	2424.141	Fe II UV180	Z3	2474.87	220	2474.762	Fe II UV208	Z3
		2424.586	Fe II UV301		2478.56	211	2478.449	Fe II UV161	rZ3
		2424.380	Fe II UV149				2478.568	Fe II UV179	
2425.71	109	2425.677	Fe II UV224?	Z	2480.22	290	2480.155	Fe II UV179	Z3
2428.47	228	2428.286	Fe II UV301	Z3	2480.98	107	2481.044	Fe II UV243	Z
		2428.367	Fe II UV300		2482.61	529	2482.117	Fe II UV161	Z3
2428.92	231	2428.795	Fe II UV301	Z3			2482.654	Fe II UV207	
2430.11	431	2430.073	Fe II UV180	Z3	2484.30	249	2484.243	Fe II UV243	Z3
		2429.382	Fe II UV148		2486.43	265	2486.343	Fe II UV208	Z3
2432.35	484	2432.259	Fe II UV180	Z3	2488.35	62			Z
2434.66	266	2434.398	Fe II UV301?	rZ3	2489.78	402	2489.485	Fe II UV161	Z3B3
2437.32	118	2437.256	Fe II UV313	Z			2489.826	Fe II UV207	
2438.12	305	2437.892	Ni II UV19?	Z3	2490.95	408	2490.856	Fe II UV179	Z3
2439.38	242	2439.301	Fe II UV209	Z3			2491.392	Fe II UV207	
2440.50	122	2440.416	Fe II UV300	Z	2493.34	455	2493.269	Fe II UV161	ZS3B3
2444.59	456	2444.515	Fe II UV148	Z3			2493.174	Fe II UV161	
2445.67	278	2445.569	Fe II UV148	Z3			2493.174	Fe II UV207	
		2445.787	Fe II UV300		2495.23	70			rZ3
2447.73	295	2447.753	Fe II UV320	Z3	2497.89	265	2497.817	Fe II UV175	Z3
2450.25	156	2450.196	Fe II UV300	Z3			2497.817	Fe II UV207	
		2449.961	Fe II UV300				2497.300	Fe II UV208	
2451.41	80	2451.208	Fe II UV209?	Z	2499.02	323	2498.897	Fe II UV161	Z3
		2451.354	Fe II UV300		2500.96	166			Z3
2454.52	221	2454.574	Fe II UV320	Z3	2502.39	298	2502.388	Fe II UV207	Z3
		2453.794	Fe II UV163		2503.93	409	2503.870	Fe II UV285	Z3
2456.93	116	2456.816	Fe II UV209	rZ			2503.560	Fe II UV161	
2457.84	33	2457.785	Fe II UV299?		2506.17	332	2506.091	Fe II UV207	Z3
2458.88	351	2458.782	Fe II UV209	Z3	2506.87	51	2506.797	Fe II UV175	3
2461.83	326	2461.282	Fe II UV209	Z3	2508.20	81			Z3
		2461.667	Fe II UV163		2509.32	87	2509.117	Fe II UV242	Z
		2461.855	Fe II UV209		2511.90	353	2511.759	Fe II UV161	Z3
2464.21	334	2464.007	Fe II UV208	Z3					
		2463.280	Fe II UV208		2514.32	290	2514.383	Fe II UV285	Z3
2464.97	482	2464.903	Fe II UV208	Z3	2517.22	152	2517.124	Fe II UV147	rZ3
		2465.194	Fe II UV148		2519.04	299	2519.044	Fe II UV268	Z3
2465.97	307	2465.911	Fe II UV208	Z3	2521.17	216	2521.089	Fe II UV268	Z3
2466.83	378	2466.811	Fe II UV179	Z3	2521.90	225	2521.810	Fe II UV330	Z3
		2466.670	Fe II UV179		2522.99	204	2522.892	Fe II UV330	Z3
2468.23	87	2468.292	Fe II UV145	Z			2522.848	Fe I UV7??	
2469.62	275	2469.512	Fe II UV299	Z3	2525.36	382	2525.386	Fe II UV159	Z3
2470.69	373	2470.661	Fe II UV179	Z3			2525.114	Fe II UV330	
		2470.752	Fe II UV223		2526.59	399	2526.292	Fe II UV145?	Z3
		2470.406	Fe II UV208		2527.33	142	2527.107	Fe II UV159	rZ3
2472.48	266	2472.426	Fe II UV179	Z3			2527.453	Fe II UV329	

Table 1: Emission Lines of 32 Cygni in Total Eclipse (page 6).

λ_{obs}	Flux	λ_{lab}	Identification	Notes	λ_{obs}	Flux	λ_{lab}	Identification	Notes
2529.57	594	2529.545	Fe II UV177	Z3	2599.5	1330	2599.395	Fe II UV1	ZsS3
		2529.545	Fe II UV145				2598.369	Fe II UV1	
2533.72	218	2533.626	Fe II UV159	Z3	2605.29	130	2605.034	Fe II UV404?	rZ3
2534.42	275	2534.413	Fe II UV159	Z3	2607.20	670	2607.086	Fe II UV1	Z3B3
2535.47	229	2535.480	Fe II UV177	Z3	2611.97	898	2611.873	Fe II UV1	ZS3B3
2536.94	356	2536.822	Fe II UV159	Z3	2613.92	628	2613.820	Fe II UV1	Z3B3
2538.97	1003	2538.794	Fe II UV158	rZ3			2613.576	Fe II UV172	
		2538.898	Fe II UV158		2617.74	616	2617.618	Fe II UV1	Z3B3
2541.08	552	2541.096	Fe II UV177	rZ3	2619.14	161	2619.071	Fe II UV171	Z3
2541.81	161	2541.831	Fe II UV158	Z3	2620.71	231	2620.693	Fe II UV171	Z3
2543.47	289	2543.382	Fe II UV159	Z3			2620.408	Fe II UV1	
		2543.431	Fe II UV177		2621.81	349	2621.669	Fe II UV1	Z3
2545.30	257	2545.432	Fe II UV267	Z3	2623.91	129	2623.721	Fe II UV171	Z3
		2545.215	Fe II UV159		2625.90	984	2625.664	Fe II UV1	ZS3B3
2546.77	201	2546.677	Fe II UV177	Z3	2628.42	612	2628.569	Fe II UV203	Z3B3
2549.23	719	2549.082	Fe II UV284	Z3			2628.291	Fe II UV1	
		2549.399	Fe II UV177		2629.67	264	2629.590	Fe II UV171	rZ3
		2549.453	Fe II UV177		2631.46	1030	2631.045	Fe II UV171	sZ3B3
2550.26	239	2550.023	Fe II UV240	Z3			2631.321	Fe II UV1	
		2550.575	Fe II UV158				2631.607	Fe II UV171	
		2550.680	Fe II UV240		2633.27	93	2633.200	Fe II UV356	Z3
2555.33	222	2555.066	Fe II UV177	Z3	2637.75	163	2637.643	Fe II UV221	Z3
		2555.447	Fe II UV177		2639.62	95	2639.560	Fe II UV221	Z3
2557.53	109	2557.500	Fe II UV175	Z3	2642.08	45	2642.015	Fe II UV309	rZ
2560.47	202	2560.278	Fe II UV221	Z3	2645.40	66	2645.328	Fe II UV426	Z3
		2559.921	Fe II UV267		2649.56	122	2649.467	Fe II UV427	Z3
2562.57	536	2562.535	Fe II UV64	Z3	2658.37	117	2658.251	Fe II UV309	Z3
		2562.094	Fe II UV221?		2664.68	350	2664.665	Fe II UV263	Z3B3
2563.60	371	2563.472	Fe II UV64	rZ3			2664.209	Fe II UV237?	
2566.89	426	2566.908	Fe II UV64	Z3	2666.67	282	2666.631	Fe II UV263	Z3B3
2568.45	155	2568.405	Fe II UV145	Z3	2669.11	29	2669.166	Al II UV1	Z3
2570.88	186	2570.843	Fe II UV284	Z3	2677.22	178	2677.19	Cr II UV8	Z3
2573.10	167	2572.965	Fe II UV190?	Z3			2677.13	Cr II UV8	
		2573.206	Fe II UV205		2678.65	110	2678.79	Cr II UV7?	Z3
2574.44	257	2574.363	Fe II UV144	Z3	2681.03	168			rZ3
2576.89	195	2576.859	Fe II UV326	Z3	2682.64	114			Z3
2577.89	254	2577.920	Fe II UV64	Z3	2684.80	264	2684.752	Fe II UV283	Z3
2581.06	190	2581.111	Fe II UV190?	rZ3	2689.25	132	2689.210	Fe II UV218	Z3
2582.67	342	2582.582	Fe II UV64	Z3	2692.78	277	2692.601	Fe II UV283	Z3B3
2586.10	630	2585.876	Fe II UV1	Z3			2692.826	Fe II UV62?	
2588.09	200	2587.945	Fe II UV326	Z3	2697.50	136	2697.453	Fe II UV341	Z
		2588.182	Fe II UV145?				2697.330	Fe II UV341	
2591.63	489	2591.542	Fe II UV64	Z3	2704.05	344	2703.988	Fe II UV261	ZS3B3
2592.85	194	2592.781	Fe II UV318	Z3	2706.84	162	2706.566	Fe II UV341	rZ3
2593.97	137	2593.722	Fe II UV64	Z					

Table 1: Emission Lines of 32 Cygni in Total Eclipse (page 7).

λ_{obs}	Flux	λ_{lab}	Identification	Notes	λ_{obs}	Flux	λ_{lab}	Identification	Notes
2709.19	211	2709.051	Fe II UV218	Z3	2781.94	159			
		2709.373	Fe II UV62		2783.76	290	2783.690	Fe II UV234	Z3B
2711.98	335	2711.842	Fe II UV201	Z3	2785.26	139	2785.213	Fe II UV373	Z3
2714.51	495	2714.414	Fe II UV63	ZS3B3	2790.92	75	2790.752	Fe II UV32	ZS3
2716.39	226	2716.216	Fe II UV261	ZS3	2796.06	1952	2795.523	Mg II UV1	sZS3B
		2716.683	Fe II UV62		2803.16	2260	2802.698	Mg II UV1	sZS3B
2719.07	134	2719.027	Fe I UV5?	Z	2805.54	61	2805.315	Fe II UV295?	
2722.03	106	2722.060	Fe II UV260	Z	2823.17	43	2823.276	Fe I UV44	fZ3
2724.82	226	2724.879	Fe II UV62	rZ3B	2831.63	71	2831.562	Fe II UV217	Z3
2727.60	479	2727.382	Fe II UV200?	ZS3B	2835.82	82	2835.63	Cr II UV5	Z3
		2727.538	Fe II UV63				2835.716	Fe II UV216?	
2729.12	71	2728.898	Fe II UV260	ZS	2839.59	51	2839.535	Fe II UV391	fZ3
2730.81	263	2730.735	Fe II UV62	Z3B	2840.67	167	2840.644	Fe II UV217	Z3
2732.35	81			Z3			2840.756	Fe II UV280	
2736.98	463	2736.968	Fe II UV63	Z3B	2843.52	102	2843.24	Cr II UV5	rZ3
2739.68	897	2739.545	Fe II UV63	ZS3B			2843.977	Fe I UV44	f
2741.46	156	2741.395	Fe II UV260	Z3	2845.54	30	2845.450	Fe II UV399	fZ3
2743.32	628	2743.196	Fe II UV62	ZS3B	2848.09	57	2848.046	Fe II UV196	Z3
2746.99	1057	2746.978	Fe II UV63	Z3B	2850.04	90	2849.83	Cr II UV5	
		2746.487	Fe II UV62		2858.44	46	2858.340	Fe II UV279	Z
2749.45	1058	2749.178	Fe II UV63	Z3B	2861.09	23	2861.187	Fe II UV61?	Z
		2749.324	Fe II UV62				2860.92	Cr II UV5?	
		2749.482	Fe II UV63		2868.79	75	2868.874	Fe II UV61	Z3
2751.05	141	2751.121	Fe II UV217	Z	2870.75	47	2870.608	Fe II UV195?	
2753.37	400	2753.289	Fe II UV235	rZS3B	2873.40	45	2873.399	Fe II UV279	Z
2755.89	1078	2755.733	Fe II UV62	Z3B	2880.81	117	2880.750	Fe II UV61	Z
2757.66	94	2757.72	Cr II UV6?	Z3	2892.78	27	2892.822	Fe II UV61	
		2757.029	Fe II UV199?		2895.33	32	2895.215	Fe II UV294?	
2759.22	92	2759.336	Fe II UV32?	Z3	2897.36	34	2897.264	Fe II UV254?	
2761.90	219	2761.813	Fe II UV63	Z3B	2926.77	111	2926.584	Fe II UV60	Z3
2762.67	77	2762.58	Cr II UV6?	Z3	2939.92	38	2939.506	Fe II UV60?	
		2762.436	Fe II UV199?		2944.51	161	2944.399	Fe II UV78	Z3
2767.67	376	2767.500	Fe II UV235	ZS3B	2947.70	171	2947.658	Fe II UV78	Z3
		2766.55	Cr II UV6?		2953.90	103	2953.774	Fe II UV60	Z3
2769.25	321	2769.354	Fe II UV198	Z3B	2970.54	72	2970.510	Fe II UV60	Z3
		2768.940	Fe II UV63		2985.03	440	2984.831	Fe II UV78	Z3
		2769.153	Fe II UV200				2985.545	Fe II UV78	
2774.77	130	2774.686	Fe II UV218	Z3	3002.67	138	3002.650	Fe II UV78	Z3
2779.35	298	2779.302	Fe II UV234	rZ3B	3010.64	178			Z3

Notes: s=saturated, r=affected by a reseau, o=at edge of an order, f=known fluorescent line, Z=observed in ζ Aur, S=listed by Stencel & Chapman (1981) for ζ Aur, 3=observed in 31 Cyg, B=listed by Bauer & Stencel (1989) for 31 Cyg. Line fluxes (Column 2) are in units of 10^{-14} ergs cm^{-2}s^{-1}.